Lasers in Eng., Vol. 0, pp. 53–65
Reprints available directly from the publisher
Photocopying permitted by license only

Laser Drilling of Microholes in Single Crystal Silicon Using Continuous Wave (CW) 1070 nm Fiber Lasers with Millisecond Pulse Widths

J.O. MACLEAN[1,*] J.R. HODSON[1], C. TANGKIJCHAROENCHAI[2], S. AL-OJAILI[2], S. RODSAVAS[2], S. COOMBER[3] AND K.T. VOISEY[2]

[1]*School of Physics and Astronomy, University of Nottingham, University Park, Nottingham, NG7 2RD, UK*
[2]*Faculty of Engineering, University of Nottingham, University Park, Nottingham, NG7 2RD, UK*
[3]*Wafer Technology Ltd., 34 Maryland Rd., Tongwell, Milton Keynes, Buckinghamshire, MK15 8HJ, UK*

The laser microdrilling of via holes in Si semiconductor wafers was studied using 1 ms pulses from an Yb fibre laser with 1070 nm wavelength. Optical microscopy and cross-sectional analysis were used to quantify hole dimensions, the distribution of recast material and any microcracking for both (100) and (111) single crystal surface semiconductor wafer orientations. The flexibility of this laser wavelength and simple pulsing scheme were demonstrated for a range of semiconductor substrates of narrow and wide bandgap including InSb, GaSb, InAs, GaAs, InP and sapphire. Detailed observations for Si showed that, between the threshold energies for surface melting and the irradiance for drilling a "thru" hole from the front surface to rear surface, there was a range of irradiances for which microcracking occurred near the hole circumference. The directionality and lengths of these microcracks were studied for the (100) and (111) orientations and possible mechanisms for formation were discussed, including the Griffith criterion for microcracks and the failure mechanism of fatigue usually applied to welding of metals. Above the irradiance for formation of a thru hole, few cracks were observed. Future work will compare similar observations and measurements in other narrow- and wide-bandgap semiconductor wafer substrates.

Keywords: Fiber laser, Ytterbium fiber laser, silicon, Si, semiconductor material, semiconductor wafer, laser drilling, percussion drilling, microcrack, pulse, Griffith criterion, via hole, thru hole, cold atoms

*Corresponding author: Tel: +44 (0)115 846 6008; E-mail: Jessica.Maclean@nottingham.ac.uk
https://orcid.org/0000-0002-8099-6981

1 INTRODUCTION

The interaction of high intensity, short laser pulses was studied for material removal from semiconductor substrates. The laser microdrilling of Si wafer single crystal substrates was investigated using a single near-infrared (NIR) laser wavelength near 1070 nm of beam waist diameter 192 μm at the substrate surface. Previous work demonstrated that a single pulse of milliseconds duration drilled thru holes of dimensions typically in the range of 200 to 500 μm diameter in materials of bandgap ranging from 1.43 eV (GaAs) to 8.90 eV (sapphire) [1]. All semiconductor substrate materials were high quality single crystal substrates suitable for epitaxial growth with a polished front surface of roughness of 2 nm and a wafer thickness in the range of 300 to 500 μm.

Under low optical intensities, photons of energies exceeding the semiconductor bandgap are absorbed; however, it is known that interfaces lead to scattering and absorption, making some nominally transparent materials opaque, and hence the successful long-wavelength laser drilling of Al_2O_3 [2,3]. For single crystal semiconductor wafers, the sub-bandgap absorption results from reduction of the bandgap due to surface melting by high optical intensity [4], impurities or structural imperfections, as well as some absorption being attributable to free carriers generated by the absorbed photons [5].

This work broadens the application of this laser drilling wavelength beyond the more common metallic materials laser drilled in industry, such as steels, and demonstrates the versatility of a single, millisecond pulse in the near-infra-red for microdrilling of thru holes in a wide range of semiconductor single crystal substrates.

2 EXPERIMENTAL TECHNIQUES

2.1 Laser details

The primary laser used was a multimode Yb fiber laser (YLR-2000; IPG Photonics Corporation), emitting a multimode beam at 1070 nm wavelength with a maximum power of 2 kW and a focused beam diameter of 192 μm. For a subset of the results a different Yb fiber laser (JK400FL; JK Lasers, Ltd.) was used which emitted a multimode beam at 1070 nm wavelength with a 400 W maximum power and a focused beam diameter of 50 μm was used, enabling smaller hole sizes to be achieved. The pulse duration was between 1 ms (the minimum duration) and a maximum duration of 10 ms, and some of the work employed two or three pulses (see Figure 1). An assist gas of Ar was used in all experiments, at a flow pressure between 0.5 and 2.0 bar, emerging concentric with the laser beam at a distance of 1 mm from the wafer surface. This directed material ejected away from the front surface of the hole, reducing spatter around the hole.

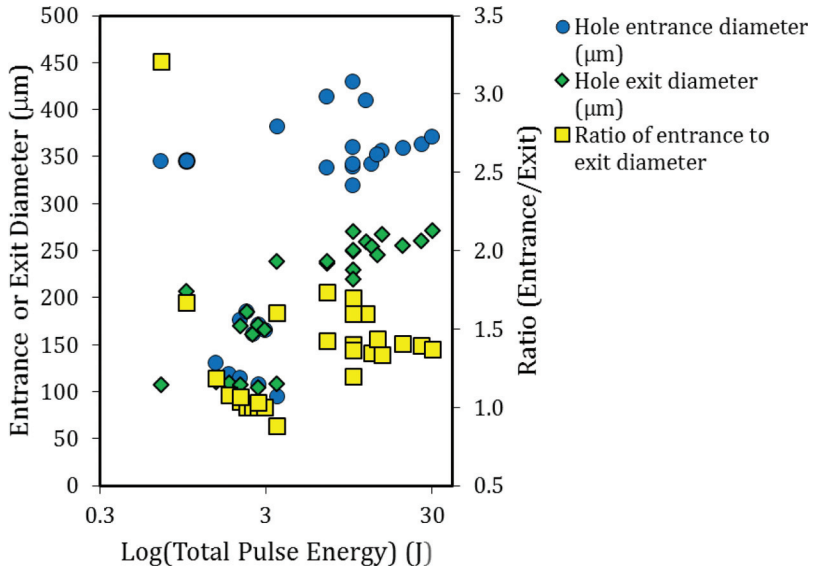

FIGURE 1
Graph showing hole entrance and exit dimensions and ratio of dimensions as a function of fibre laser pulse energy for holes laser drilled in Si wafers at 1070 nm for different pulse sequences and the two different lasers used.

2.2 Materials details

This investigation used a range of semiconductor materials with different fundamental material parameters in order to assess the suitability of near-infra-red (NIR) fiber lasers for the processing of semiconductor wafers. Si wafer substrates were commercially-sourced "epi-ready" process trial semiconductor substrate wafers of 50 mm diameter (Wafer Technology, Ltd.) of typical root-mean-square surface roughness, R_{rms}, of 2 nm on the epi-ready side and R_{rms} of 2.0 µm on the rear side. Previous work demonstrated the importance of surface roughness in the entrance hole dimension and compared the difference between the entrance and exit diameters of holes for different substrate materials (sapphire, GaAs, Si) also using a wavelength of 1070 nm and a laser irradiance in the range of 1.7×10^6 to 1.1×10^7 W/cm^2 [1]. We describe here the overall results for the laser drilling of Si in terms of hole dimension achieved (see Figure 1). A dependence of microcracking on irradiance was identified.

2.3 Sample preparation and analysis

The principal drilling parameters of power, pulse length, number of pulses, focal position, wafer orientation were varied to achieve holes of a range of dimensions through single crystal Si (room temperature bandgap 1.1 eV) using the 1070 nm wavelength and a minimum pulse length of 1 ms. Optical

microscopy was carried out using optical microscopes (Eclipse LV100ND; Nikon Corporation and MX51; Olympus, Ltd.) for the assessment of hole dimensions and hole shape (see Figure 2), crack lengths and directions, and recast material location. The associated materials damage was assessed post-laser drilling, including the area known (for metals) as the heat affected zone (HAZ), the location of recast material, the reproducibility of the average hole dimension and any microcracking which may result from mechanical stress [6]. An assessment of the visible total crack length on the surface and the orientation relative to the major crystallographic directions was made (see Figure 3 and Figure 4). Having investigated the robustness for larger diameter holes (see Figure 5), we demonstrated our first application to an atom chip, as an aperture for optical access and as an orifice for differential pumping under ultra-high vacuum (UHV) conditions (see Figure 6) and no further process steps were required for the hole other than solvent cleaning.

Substrates were placed with the highly polished face a few degrees from the normal to the fibre laser beam which was focused on the substrate surface for Si (100) (see Figure 7(a)) and Si (111) (see Figure 8(a)) with some further experiments made focusing 0.5 mm and 1 mm below the surface for Si (100) (see Figure 7(b) and Figure 7(c)) and for Si (111) (see Figure 8(b) and Figure 8(c)). Samples were mounted a few centimetres above the translation stage resting on a ring-shaped ledge of a precision-machined, cylindrical stainless steel cylindrical holder. We focus here on the presentation of our results of microholes in Si following the analysis of hundreds of holes, laser-drilled under different parameters.

The next step of a device reliability assessment would be dependent on the application. For example, in an application of a *via* hole as an "emitter wrap

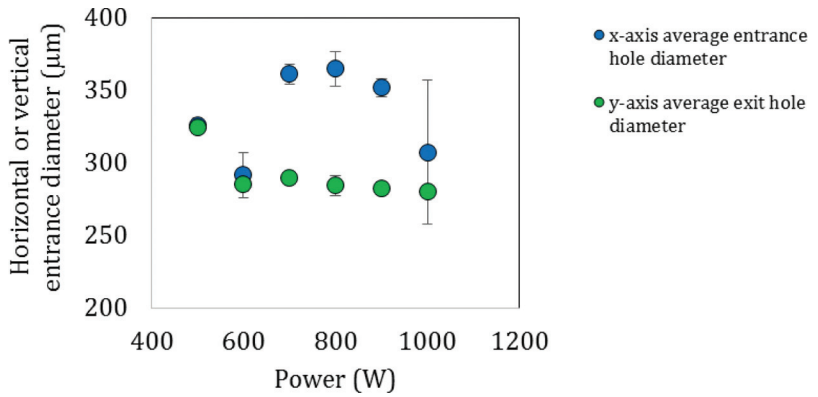

FIGURE 2
Graph showing the dimensions of entrance holes in orthogonal directions <100> and <010> for Si (100) as a function of laser power for a fibre laser beam diameter of 192 µm when laser drilled at an Ar assist gas pressure of 0.5 bar. Each data point shows the mean of a set of five identical holes for each parameter set.

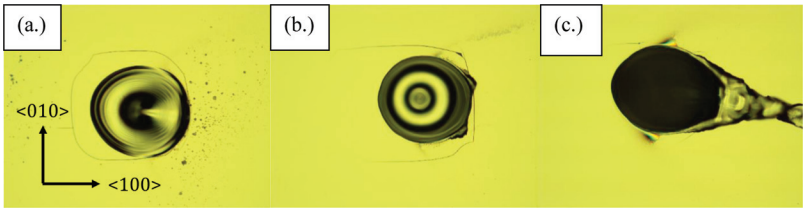

FIGURE 3
Optical micrographs showing the threshold energy of 0.5 J for fibre laser microdrilling an epitaxial Si (100) wafer for a 1 ms pulse at 1070 nm wavelength and exhibiting concentric ripples, possibly similar to the Marangoni effect and associated microcracking following the principal crystallographic directions, at (a) 500 W, (b) 600 W and (c) 700 W. Holes were approximately 300 µm in diameter. No sample cleaning was performed post-drilling.

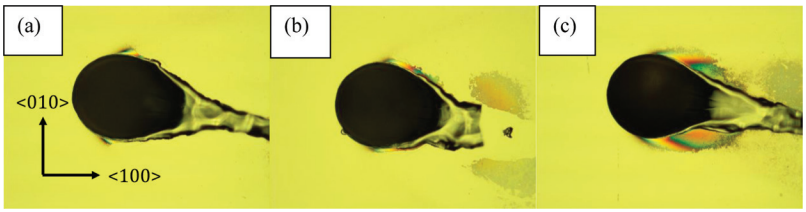

FIGURE 4
Optical micrographs of holes of approximately 300 µm diameter in Si(100) using (a) 800 W, (b) 900 W and (c) 1000 W power for 1 ms at 1070 nm wavelength showing re-solidified melted Si and very few microcracks. No sample cleaning was performed post-drilling.

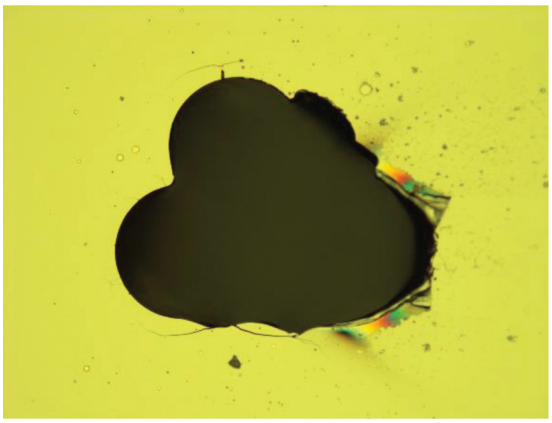

FIGURE 5
Optical micrograph of a hole of approximately 600 µm diameter fibre laser microdrilled in a Si wafer by drilling three holes 200 µm apart at 700 W for 1 ms. The hole was approximately triangular and exhibited a few short cracks approximately parallel to and originating from the hole circumference. No sample cleaning was performed post-drilling.

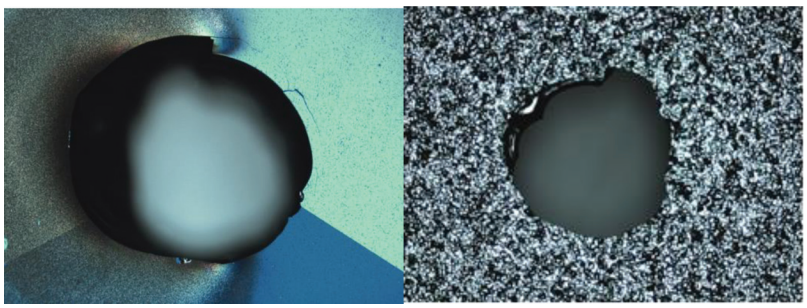

FIGURE 6
Optical micrographs of the entrance (left hand side) and exit (right hand side) of a hole of approximately 550 µm diameter fibre laser microdrilled in the centre of a patterned Si wafer by drilling a single hole at 1400 W for 2 ms with a laser beam diameter of 400 µm. The hole was approximately circular and exhibited relatively short length of cracks approximately parallel to, and originating from, the hole circumference.

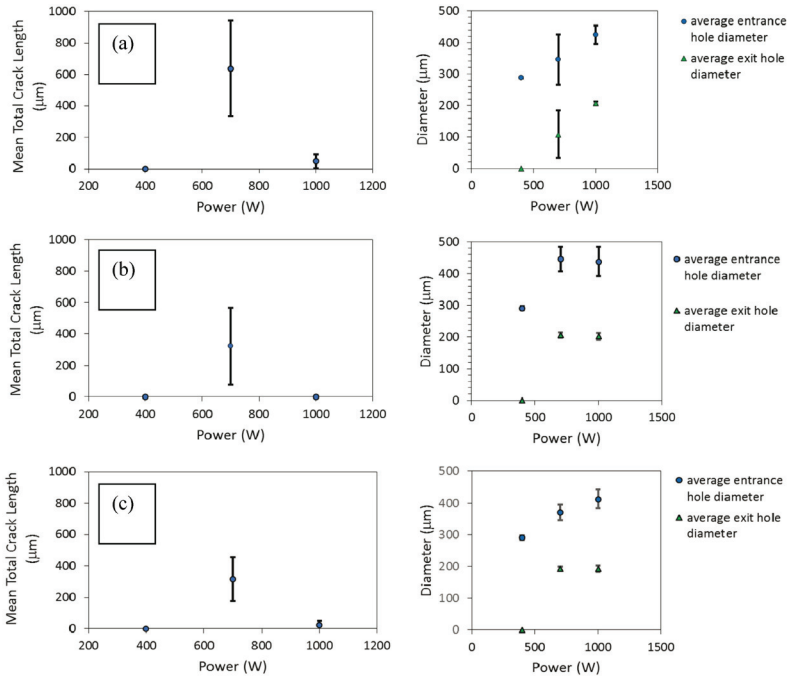

FIGURE 7
Measurements from the optical microscopic analysis of holes in Si (100) microdrilled at an Ar assist gas pressure of 0.5 bar at different focal positions with respect to the wafer surface of (a) surface, (b) -0.5 mm and (c) -1.0 mm, revealing cracks at intermediate powers. The graphs show the total crack length and the hole entrance (blue) and exit (green) dimensions as a function of laser power at 400, 700 and 1000 W. Each data point is the mean of a set of five identical holes under each set of parameters.

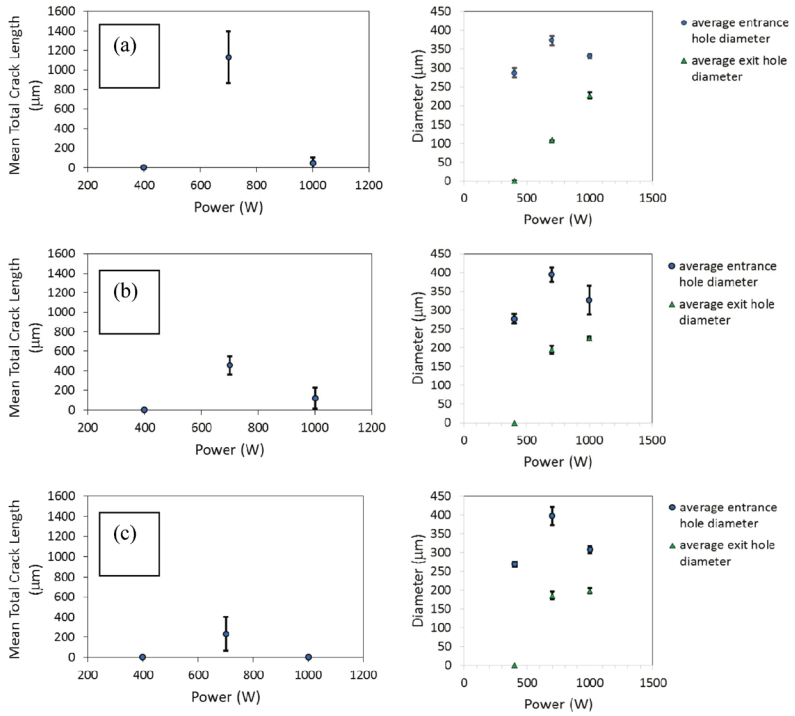

FIGURE 8
Measurements from the optical microscopic analysis of holes in Si (111) microdrilled at an Ar assist gas pressure of 0.5 bar, at different focal positions with respect to the wafer surface of (a) surface, (b) -0.5 mm and (c.) -1.0 mm, revealing cracks at intermediate powers. The graphs show the total crack length and the hole entrance (blue) and exit (green) dimensions as a function of laser power at 400, 700 and 1000 W. Each data point is the mean of a set of five identical holes for each parameter set.

thru" contact, an assessment of surface leakage current from the short circuit current would be important for a solar cell device [7].

3 SIMPLE LASER DRILLING MODEL

In laser drilling the energy deposited into the material is partially absorbed, initiating melting and further increasing absorption causing vaporization, expansion of a gaseous plasma and melt ejection.

A simple calculation, based on data in Table 1, predicting the energy required for melting and vaporization, E, was employed, which is the energy required to remove a typical cylindrical volume of the single crystal Si of diameter 250 µm in terms of melting followed by vaporization:

TABLE 1
Thermodynamic parameters and material properties of single crystal Si used to estimate the energy required to drill a microhole of 250 μm diameter by melt ejection.

Material Property	**Data for Si**
Bandgap at 300 K, E_g	1.12 eV
Specific heat capacity, Cp	712 J/Kkg
Latent heat of vaporization, L_v	1926 kJ/kg
Latent heat of melting, L_m	1.42×10^6 J/kg
Melting point, T_m	1410°C
Density, ρ	2330 kg/m^3
Energy requirement, E (J) (estimated from Equation (1))	249 mJ
Laser pulse energy at maximum power, P	2.0 J

$$E(J) = m(Cp\ \Delta T + Lm + Lv) \tag{1}$$

where m is the mass of material removed, ΔT is the temperature change, C_p is the specific heat capacity at constant pressure, L_v is the latent heat of vaporization, L_m is the latent heat of melting, E_1 is the threshold energy for piercing the surface and E_2 is the threshold energy for a "thru" hole.

Equation (1) suggests that a single pulse of 1 ms at the maximum (peak) power of 2 kW should exceed the energy required by a factor of eight. This simple model, however, does not account for the thermal diffusivity of the materials and the extent of the area affected by rapid surface heating. There is the potential for a brittle material to crack as the result of rapid differential thermal expansion and contraction. The Griffith criterion predicts that a crack will propagate when a tensile stress is applied if the crack propagation results in a decrease in elastic strain energy which exceeds the increase in surface energy due to the surface area of the crack [6].

4 RESULTS

Figure 1 shows a collation of data for the diameter, in microns, of the entrance and exit holes as a function of total pulse energy for holes drilled in Si wafers, using different pulse repetitions and durations. The total pulse energy was in the range from 1.0 J (1000 W for 1 ms) to 30.0 J (1500 W for 10 ms and two pulses). At large total pulse energies the ratio of the entrance to exit diameter remained in the range 1.3 to 1.4 with the entrance diameter having a value around 350 μm and an exit around 250 μm. At lower energies, when using the JK400FL fibre laser, of beam waist diameter 50 μm, the hole dimensions depended strongly on total energy with a strong decrease in hole dimension

with increase in energy, decreasing from 400 to 120 μm as the energy changed from 1.0 to 3.0 J. The corresponding ratio of entrance to exit diameter was lower in this energy range, reaching less than one and corresponding to an enhanced exit diameter with respect to the entrance diameter. The cross-sectional taper of the hole changed from positive, to cylindrical, to a negative taper. It may be seen from Figure 1 that a wide range of hole dimensions and cross-sections was achieved.

The entrance hole dimensions are shown in Figure 2 as a function of laser power for a single 1 ms pulse when using the full 2 kW output of the IPG fiber laser. At the threshold for surface melting the hole was circular and then became elliptical until it was circular again when a thru hole was made.

Figure 3 and Figure 4 show plan-view images of holes of approximately 300 μm in diameter fibre laser drilled in Si (100). The morphology of the hole evolved as a function of power showing the effects of melting, vaporization and resolidification.

Investigations were also made to achieve increased hole diameter including the use of closely spaced holes to achieve a larger orifice. Such an orifice is shown in Figure 5 and was laser drilled using 1 ms pulses at 700 W with a hole spacing of 0.2 mm, resulting in a hole of approximately 600 μm diameter. Short (<100 μm) lengths of cracks were observed which were approximately parallel to the circumference of the overall hole.

In order to demonstrate the compatibility of the fibre laser microdrilling technique with semiconductor wafer nanofabrication techniques used for the components of a cold atom quantum sensor, the laser drilling technique was applied to a Si wafer which had already been patterned and dry-etched with a diffraction grating designed for 780 nm laser light [8]. Figure 6 shows optical microscopy of the hole which was located in the centre of the pattern using a precision translation stage below the laser-drilling beam. The hole diameter was 550 μm and the exit diameter was 450 μm. The subsequent successful achievement, under vacuum conditions, of a cloud of magneto-optically trapped Rb cold atoms a few millimetres above the hole demonstrated that the presence of the hole did not adversely affect the optical trapping. This also confirmed that the spattered material was successfully removed from the patterned surface by standard solvent cleaning techniques.

Two different and technologically important wafer orientations of Si, (100) and (111), were compared in terms of the total crack length as a function of power and the hole dimensions achieved. The entrance and exit hole diameters were plotted at three irradiances: 400 W or 1.4×10^7 J/m^2; 700 W or 2.4×10^7 J/m^2; and 1000 W or 3.5×10^7 J/m^2), as were the total crack lengths (see Figure 7 and Figure 8). The drilling threshold corresponded to 0.4 J of energy for both wafer orientations. There was an intermediate irradiance, between the onset of drilling and the achievement of a thru hole, which exhibited cracks around the hole. In this intermediate region the dimension of the hole increased as a function of power and then the dimension tended to

reach a plateau. Above the threshold for drilling through the wafer, few cracks resulted. The focus of the fibre laser beam was changed from the wafer surface to 0.5 mm (see Figure 7(b) and Figure 8(b)) and 1.0 mm below it (see Figure 7(c) and Figure 8(c)) and the same parameters were measured. The intermediate region was present at all three focal lengths and the crack length and hole dimensions were similar.

The dimensional and microcrack length data in Figure 7 and Figure 8 for the (100) and (111) orientations of Si were similar. There was no significant change in crack length for the three focal distances and the cracks were negligible in total length at the irradiance for which the thru hole was more cylindrical. The hole dimensions of (100) and (111) orientations were similar and appeared to tend to a plateau at high power suggesting that the leading edge of the pulse determined the melt ejected volume and that the diameter did not evolve during the duration of 1 ms, or indeed with the number of pulses, as previously mentioned for Figure 1. The intermediate region in which many cracks were generated may correspond to a regime in which the temperature gradient causes the tensile strength to be exceeded and fracture occurs.

The results generally demonstrate the similar behaviour of the melt threshold and thru hole thresholds for the different wafer orientations of Si. Further examination of the morphology of the drilled holes in the two wafer orientations shown in Figure 3 and Figure 4 will be made in future work.

5 DISCUSSION

The melt ejection mechanism expels material by the pressure of a vaporized gaseous plasma exiting the hole and this mechanism was observed for all laser drilling parameters used in this study. The computational modelling of these physical processes was carried out by Verhoeven *et al* [9]. This contrasts with the work of Yu *et al* [4], in which a similar wavelength of light was used to remove Si using femtosecond pulses in an ablation process which relied on maintaining a thermal equilibrium between thermal diffusion and incident optical energy, to provide a high temperature gradient at the melted surface.

In our study of single crystal Si, the laser drilling exhibited a threshold for absorption of the NIR radiation and melting the Si surface. On increasing the laser power, the hole showed some ellipticity (see Figure 2) and the hole cross-section evolved from a positive taper, until at a high power threshold, a cylindrical and circular thru hole was obtained (Figs. 3 and 4). Further increase of the power resulted in little further increase in dimension for a single pulse. In this study the threshold for absorption was 0.4 to 0.5 J and the high power threshold was 1.0 to 1.1 J for a 280 to 340 μm diameter hole when the beam waist was 192 μm, for both (100) and (111) substrates.

When more material was melted than was ejected forward through the hole, a plume of melted and solidified Si was present on the surface, directed away from the hole (see Figure 3(c) and Figures 4(a) to (c)). The removal of this solid with subsequent solvent cleaning revealed a symmetrical HAZ around the entrance to the hole.

Optical microscopy of the less heated region surrounding the melted, ejected material revealed changes on increasing the laser power. At the threshold for surface melting, there was some re-solidification of melted Si around the circumference of the entrance hole, similar to the kerf resulting from laser welding. At higher powers, as the hole deepened, the re-cast material was located on the hole sidewalls. Following cleavage and mounting in a thermosetting resin, this material survived the polishing process to reveal the interior sidewalls of the hole indicating that the recast grain boundaries were not significantly weakened.

Above the threshold for melting, the entrance holes showed microcracks originating at the hole circumference, some of which bifurcated and counter-propagated, being parallel to the hole circumference, or the major crystallographic directions, at a distance of tens of microns typically. This distance increased at very high energies (exceeding 10.0 J). The total crack length also increased with the power initially and then decreased towards a high power threshold (as in Figure 7 and Figure 8). More recent studies suggested that the total crack length then increased monotonically beyond a high power threshold. We observed that a high power threshold corresponded to a minimum in the micro cracking in the heat affected area and a fully melt ejected hole.

As a result of these observations and measurements, a simple conceptual model emerged, of a lower energy threshold for surface melting and a higher energy threshold, a high power threshold, for the fabrication of a thru hole, with an intervening morphology characterized by circumferential micro cracking in the HAZ, rising to a maximum and falling between these values. Measurements above a high power threshold showed a weak variation in hole dimension and indicated that micro cracking was a gradually increasing function of pulse energy, increasing at a rate of about 50 μm/J.

It was assumed that the wafers exhibited no intrinsic residual stress before laser-drilling but this has not yet been confirmed experimentally. Raman spectroscopy was applied to demonstrate changes in residual stress of Si after laser cutting of Si die [10].

The microcracking may be analogous to the fatigue failure seen in the welding of metals [11]. Cyclic loading of welds subjects the weld to an oscillating stress over time, resulting in both tensile and compressive forces causing the metal surface to exhibit intrusions and extrusions along slip planes. The maximum Si crack width measured by optical microscopy was 1.3 μm for a hole diameter of 250 μm.

Our results, achieving a wide range of hole dimensions, demonstrate both the control of hole dimension and the minimization of associated microcrack-

ing. We propose that an excess of energy beyond the threshold for achieving a thru hole causes a tensile stress which is sufficient to generate microcracks in the area around the entrance hole of the Si. Further investigations, such as high-speed imaging, may be necessary to determine the factors determining the initial crack locations. It is possible that melted material which remains at the hole entrance plays some role in reducing crack initiation.

6 CONCLUSIONS

The ability to rapidly drill through hundreds of microns of material and locate a hole of sub-mm dimensions precisely, in a brittle substrate such as a semiconductor wafer is a novel capability. Yb fiber lasers of wavelength 1070 nm were used with maximum power of 2 kW and beam diameter of 192 μm, or, alternatively, a 400 W Yb fiber laser of beam diameter 50 μm. Holes of diameters between 70 and 600 μm were achieved in Si. Long (ms) pulses were shown to be effective for these brittle semiconductor materials in contrast to the necessity of ultra-short pulses in many reports.

When using the minimum pulse length of 1 ms, the pulse energy thresholds were established for piercing a hole in both (100) oriented and (111) oriented Si. An investigation of the differences between the (100) and (111) orientations of Si were made. For both crystallographic orientations, observations and measurements were consistent with a simple conceptual model of the presence of microcracks around the holes in Si within a critical irradiance range between the energy threshold for surface melting and the energy threshold for drilling of a thru hole. Beyond the energy necessary for fabricating a thru hole there was some evidence that at high pulse energies (>10.0 J) there was a further increase in total crack length. Both substrates showed a minimum in total crack length near the upper threshold. The non-pierced holes exhibited surface ripples of solidified melted Si similar to the Marangoni effect and this is under further investigation. Similar trends were observed when the laser was defocused to −0.5 mm and −1.0 mm beneath the wafer surface. The hole dimensions and cross-sectional shape were relatively unchanged beyond the upper threshold, illustrating that the correct choice of parameters may access a tolerant region for a manufacturing process.

Future work will investigate whether there are any requirements for the epitaxial structure or surface passivation of the hole in order to incorporate this fabrication step into the process flow of a semiconductor device such as a photodetector or solar cell. This could be studied by making electrical measurements of appropriately designed surface leakage and bulk leakage structures.

Importantly, these results demonstrate that elaborate pulsing schemes at ultraviolet (UV) wavelengths for material ablation are not essential for the production of microholes in semiconductor substrates. The holes achieved so

far are of sufficient quality for a mechanical aperture (e.g. as a hole of specific vacuum conductance) or in order to provide optical access for optical tweezing or trapping of ultracold atoms or ions, say. The 1070 nm wavelength is flexible for laser drilling in manufacturing processes for a range of materials.

ACKNOWLEDGMENTS

This work is funded by the Engineering and Physical Sciences Research Council (EPSRC) through the UK Quantum Technology Hub for Sensors and Metrology, SM-30535 EP/M013294/1. J.O. Maclean wishes to thank S. Branston for technical assistance.

REFERENCES

[1] Maclean J.O., Hodson J.R. and Voisey K.T. Laser drilling of via micro-holes in single-crystal semiconductor substrates using a 1070 nm fiber laser with millisecond pulse widths. *Proceedings of the SPIE* **9657** (2015), 965704-1-6.

[2] Hanon M.M., Akman E., Oztoprak B.G., Gunes M., Taha Z.A., Hajim K.I., Kacar E., Gundogdu O. and Demir A. Experimental and theoretical investigation of the drilling of alumina ceramic using Nd:YAG pulsed laser. *Optics & Laser Technology* **44**(4) (2012), 913–922.

[3] Beyer H., Ross W., Rudolph R., Michaelis A., Uhlenbusch J. and Viol W. Interaction of CO2-laser pulses of microsecond duration with Al_2O_3 ceramic substrates. *Journal of Applied Physics* **70**(1) (1991), 75–81.

[4] Yu K.X.Z., Wright L. G., Webster P.J.L. and Fraser J. M. Deep non-linear ablation of silicon with a quasi-continuous wave fiber laser at 1070 nm. *Optics Letters* **38**(11) (2013), 1799–1801.

[5] Ambacher O., Rieger W., Ansmann P., Angerer H., Moustakas T.D. and Stutzman M. Sub-bandgap absorption of gallium nitride by photothermal deflection spectroscopy. *Solid State Communications* **97**(5) (1996), 365–370.

[6] Smallman R.E. and Ngan A.H.W. (Eds.) *Modern Physical Metallurgy*. Berlin: Elsevier. 2014.

[7] Ahn S., Huang D.J., Park H.K. and Grigoropoulos C.P. Femtosecond laser drilling of multicrystalline silicon for advanced solar cell fabrication. *Applied Physics A: Materials Science & Processing* **108** (2012), 113–120.

[8] Nshii C.C., Vangeleyn M., Cotter J.P., Griffin P.F., Hinds E.A., Ironside C.N., See P., Sinclair A.G., Riis E. and Arnold A.S. A surface-patterned chip as a strong source of cold atoms for Quantum Technologies. *Nature Nanotechnology* **8** (2013), 321–324.

[9] Verhoeven J.C.J., Jansen J.K.M., Matheij R.M.M. and Smith W.R. Modelling laser-induced melting. *Mathematical and Computer Modelling* **37** (2003), 419–437.

[10] Di Basio M., Kraft, M., Roesner M., Bergmann C., Cerezuela-Barreto M., Lewke D. and Schellenberger M. Direct optical stress sensing in semiconductor manufacturing using Raman micro-spectrometry. *15th IEEE Sensors Conference*. 30 October – 3 November 2016, Orlando, FL., USA. pp. 88–99.

[11] Cottrell A.H. and Hull D. Extrusion and intrusion by cyclic slip in copper. *Proceedings of the Royal Society A: Mathematical, Physical and Engineering Sciences* **242**(1229) (1957), 211–213.